PPPL-2177

UC20-F,G

I-18950

PPPL-2177

DR-0732-3

PARASITIC EXCITATION OF ION BERNSTEIN WAVES FROM A FARADAY SHIELDED FAST WAVE LOOP ANTENNA

By

F. Skiff, M. Ono, P. Colestock, and K.L. Wong

DECEMBER 1984

PLASMA PHYSICS LABORATORY

PRINCETON UNIVERSITY
PRINCETON, NEW JERSEY

PREPARED FOR THE U.S. DEPARTMENT OF ENERGY,
UNDER CONTRACT DE-AC02-76-CHO-3073.

PARASITIC EXCITATION OF ION BERNSTEIN WAVES FROM A FARADAY SHIELDED FAST WAVE LOOP ANTENNA

F. Skiff†, M. Ono, P. Colestock, and K.L. Wong

Plasma Physics Laboratory, Princeton University
Princeton, New Jersey 08544

PPPL--2177
DE85 005352

ABSTRACT

Parasitic excitation of ion Bernstein waves is observed from a Faraday shielded fast wave loop antenna in the ion cyclotron frequency range. Local analysis of the Vlasov-Maxwell equations demonstrates the role of plasma density gradient in the coupling process. The effects of plasma density and of parallel wave number on the excitation process are investigated.

†F. Skiff supported by Fannie and John Hertz Foundation fellowship.

Fast wave heating in the ion cyclotron frequency range has proven to be an effective means of heating laboratory plasmas.[1] Due to the importance of this means of heating for thermonuclear fusion experiments and of the possibility of other applications for the fast wave (e.g., current drive), it is important to understand the physics of wave coupling so that appropriate antennas may be designed for these applications. In particular, the role played by the slow wave in fast wave coupling is considered here. Generally, it is assumed that the presence of a Faraday shield will suppress the excitation of slow waves from a fast wave polarized antenna. The ion Bernstein wave and/or anomalous ion heating is observed, however, in fast wave experiments and it is uncertain whether or not this is due to direct parasitic excitation.[2,3]

In this paper we report the observation of parasitic ion Bernstein wave (IBW) excitation from a Faraday shielded fast wave loop antenna in ACT-I. The effects of plasma density and parallel wave number on this process are investigated. Local analysis of the Vlasov-Maxwell equations is used to demonstrate the effect of the plasma density gradient. At high density ($N_e \sim 10^{11}$ cm^{-3} at the edge) the parasitic loading is strong, coupling over 90% of the power from a 0.25 Ω antenna circuit. In fact, the efficiency of IBW excitation seen in this experiment is only slightly lower than that obtained with B_Θ loops.[4] Parasitic excitation of ion Bernstein waves may alter the profile of power deposition in fast wave experiments.

Since the coupling of wave energy to plasmas generally occurs at the surface of a plasma filled region, solution of the coupling problem involves consideration of a strongly inhomogeneous plasma. In contrast to nearly uniform plasmas where one has distinct modes except near degeneracies of mode wavelengths (mode conversion), the presence of a density gradient with a scale length comparable to locally defined mode wavelengths generally invalidates the solution of plasma wave equations in terms of distinct modes (wavelengths). Starting from the Vlasov-Maxwell equation

$$\nabla \times \nabla \times E + K\{E\} = \frac{4\pi i \omega}{c^2} J_A \tag{1}$$

where J_A is the current density representing the external coils and K is the warm plasma dielectric tensor (differential operator), which was derived by the procedure of Colestock, the most important warm plasma contribution enters through K_{xx} with $K_{xx} = K_{xx}^c + K_{xx}^W$.[5] K_{xx}^c is the cold plasma dielectric element. K_{xx}^W is the warm plasma contribution kept to first order in ρ_i^2

$$K_{xx}^W = -\partial_x \left\{ \frac{3\omega_{pi}^2 \, \Omega_{ci}^2 \, \rho_i^2}{(4\Omega_{ci}^2 - \omega^2)(\omega^2 - \Omega_{ci}^2)} \right\} \partial_x ,$$

where the derivatives act on everything to the right. For regular points of Eq. (1), the six parameter family of solutions can be constructed locally from the indicial equations:

$$-K_{xx}^w(o)\,(m+2)(m+1)\,E_x^{(m+2)} - K_{xx}^w(1)\,(m+1)^2\,E_x^{(m+1)}$$

$$+(K_{xx}^{c(o)} - k_y^2 - k_z^2)E_x^{(m)} + K_{xx}^{c(1)} \; E_x^{(m - 1)} =$$

$$-K_{xy}^{(o)}E_y^{(m)} + i(m + 1)k_y E_y^{(m + 1)} + i\,(m + 1)k_z E_z^{(m + 1)} - K_{xy}^{(1)}E_y^{(m - 1)}$$

$$(m + 2)\,(m + 1)\,E_y^{(m + 2)} + (K_{yy}^{(o)} - k_z^2)\,E_y^{(m)} + K_{yy}^{(1)}\,E_y^{(m - 1)} =$$

$$-K_{yz}^{(o)}\,E_x^{(m)} - K_{yx}^{(1)}\,E_x^{(m -1)} + ik_y(m + 1)\,E_x^{(m + 1)} - k_y k_z E_z^{(m)}$$

$$(m + 2)\,(m + 1)\,E_z^{(m + 2)} + (K_{zz}^{(o)} - k_y^2)\,E_z^{(m)} + K_{zz}^{(1)}\,E_z^{(m - 1)} =$$

$$ik_z(m + 1)\,E_x^{(m + 1)} - k_y k_z E_y^{(m)}\;,$$

where the electric field components have been expanded as $E_i(x) = \sum_n E_i^{(n)} x^n$ and the dielectric elements as $K_{ij} = K_{ij}^{(o)} + K_{ij}^{(1)} x$. The six free parameters can be taken to be $E_x^{(o)}$, $E_x^{(1)}$, $E_y^{(o)}$, $E_y^{(1)}$, $E_z^{(o)}$, and $E_z^{(1)}$. Also, $E_i^{(n)} = o$ for $n < o$. In uniform regions, solutions consist of the wave solutions of the 6^{th} order system (the characteristic equation has three roots in k_x^2).

Since the coupling problem is determined primarily by properties of the system in the antenna near field, a simple model which resembles the experimental situation is used. We model the coupling problem with the situation shown in Fig. 1. Three regions exist in the slab model with y and z being ignorable coordinates (the toroidal magnetic field is along z). The first (I) is a low density region between the conducting wall and the antenna sheet current (width d1). The second (II) is a region where the plasma density increases linearly. This region starts at the antenna and continues in the x direction a distance d2. The third (III) is a semi-infinite uniform slab which begins at the end of the ramp. Local analysis of Eq. (1) in the ramp region (II) provides a solution which can be connected to the appropriate solutions in the uniform regions (I,II). The connection is performed using continuity constraints on the fields derived from the governing Eq. (1). The most realistic results are obtained when one assumes that short wavelength modes in region I incident on the wall are absorbed whereas long wavelength modes are reflected. Reflective short wavelength modes produce coupling resonances not seen in the experiments. The Faraday shield is simulated by removing the field constraints on E_x at the antenna and constraining E_z to be zero.

Figure 2 shows some of the results of the above model. Shown in Fig. 2 is the predicted radiation resistance on the ACT-I antenna (described later) from the ion Bernstein wave with $k_z = 0.01$ and with flat density profiles, $N_e^{I} = N_e^{III} = 10^9$-$10^{11}$. Because of the Faraday shield and because of the low surface impedance of the IBW, the power coupled is very low in the absence of a density gradient. Figure 2b is like 2a except that $N_e^I = 10^9$ and $N_e^{III} = 10^9 - 10^{11}$ which provides a density gradient. In this case the coupling is several orders of magnitude larger. It is evident that, although in uniform plasma the Faraday shield inhibits slow wave excitation, a density gradient in the antenna near field can defeat the effect of a Faraday shield. Figure 2a shows the effect of changing the parallel wave number kz on the IBW from an antenna monochromatic in kz. Maximal coupling is obtained when kz is adjusted such that k_x^2 (fast wave) = 0. As density increases, therefore, so does the optimal value of kz. In this parameter condition, changes in density more readily affect wave characteristics (wave number and polarization) producing intermode coupling. The effect of changing d2 is somewhat dependent on the values of the other parameters. Figure 2d shows the effect of changing d2 (d2 $\cdot\, k_x^{IBW}$ average = 0.75-7.5) Consideration of gradients with $d2/\rho_i < 1$ where ρ_i is the ion gyroradius (0.3 mm here) would violate assumptions in the derivation of K (the dielectric), and would be too sharp to obtain experimentally as well. A different analysis is necessary to show the connection to the weak gradient limit ($k_x d_z \gg 2\pi$) where coupling is weak.[6]

A physical argument for density gradient enhanced coupling can be given as follows. In the context of the slab model, a fast wave antenna produces an electromagnetic E_y field at the plasma surface. Plasma electrons and ions respond to this field with $E \times B$ directed motions which, in the ion cyclotron frequency range ($\Omega_i < \omega \ll \Omega_e$), are oppositely directed and comparable in magnitude. In the presence of a plasma density gradient the particle excursions result in charge separation and consequent (through the Poisson equation) E_x field. It is this E_x field which drives the ion Bernstein wave. In other words, the spatial derivative $\partial_x K_{xy}$ enables the ion Bernstein wave to couple through E_y.[6]

The experimental investigation of this excitation process was performed on the ACT-I research torus. ACT-I has a 59-cm major radius, 10-cm minor radius, and a toroidal field adjustable from 1-5 kG on the minor axis. The hydrogen plasma with density 10^9-10^{12} was produced by an electron beam from either a biased hot filament source or from a carbon-heated lanthanum hexaboride cathode (for higher density range).[7] Plasma temperatures of $T_e \sim T_i \sim 2$ eV and low collisionality $\nu_i/\Omega_i \sim 10^{-3}$-$10^{-4}$ were typical.

The experimental set up is shown in Fig. 3. A set of two Faraday shielded ICRF fast wave loop antennas were excited either in phase or 180° out of phase by means of a matching network. Each loop consists of an end-fed copper bar which is bent so as to subtend approximately 60° of poloidal angle. Excitation of waves was observed directly using rf probes and a spectrum analyzer or lock-in amplifier. It was possible, as well, to monitor the power coupled from the antenna though the consequent loading of the antenna circuit. A Rogowski loop on the antenna feed provided this information. Excitation of the ion Bernstein wave was evident from the probe data. Both the sign (Fig. 4a) and magnitude (Fig. 4b) of the wave number k_x obtained from interferometry are that of the IBW. Since the antenna height h was such that $k_x \cdot h \gg 1$, the wave fronts indicate very little diffraction in the poloidal plane (Fig. 4c). With increasing density the antenna loading was observed to increase. Figure 5a shows percent power coupled vs N_e (edge) from the 0.25 Ω antenna circuit as solid curves. The density is that evaluated at the same radius as the antenna using an interferometer as well as Langmuir probes. The prediction of the theory (dotted line) is shown for comparison. Two different density profiles were used, corresponding to the two means of producing the electron beam. The lanthanum cathode tends to produce a more square profile (Fig. 5b). The filament produces a more level gradient (Fig.

5c). The effect of changing the k_z spectrum is shown in Fig. 6. Figure 6a shows the resulting antenna loading resistance for 0° relative phasing of the antennas and Fig. 6b shows the result for 180° relative phasing. In each case the data are compared to the model results for estimated k_z spectra.

Since coupling increases with density, the model suggests that coupling should degrade with increasing wave number. This is because the antenna spectrum is predominantly above the optimum in Fig. 2c. The discrepancy in Fig. 6b may indicate that 180° phasing has more long wavelength components than we suspect on the basis of Fourier analysis of the antenna structure.

Wave amplitude (derived from interferograms) also indicates that radiated IBW power increases with density. Figure 7 shows the radial amplitude-envelope at several densities. For constant wave power one would expect the wave amplitude to scale as $(N_e k_x)^{-1/2}$. Rather than being decreased by a factor of what is 3 over this density range, the amplitude actually increases with density. This indicates that the coupling does indeed increase faster than linearly with density. A more quantitative inference from the probe data requires a consideration of the wave trajectory. In particular, although the coupling is worse for 180° phasing, the probe data indicate a larger amplitude since the larger k_z components have a more toroidal trajectory and thus more readily reach the probe. Interferograms over the poloidal plane (Fig. 7a) when compared to density contours (Fig. 7b) indicate preferential coupling in regions of larger gradient. The same effect is evident in the two sets of curves of Fig. 5.

In summary we have presented observations of parasitic excitation of ion Bernstein waves from a Faraday shielded fast wave antenna. The dependence on plasma density and on parallel wave number is investigated. Parallel wavelengths which correspond to the fast wave cutoff are preferred by the coupling mechanism. A simple model is presented which accounts for the observed excitation in terms of the effect of a plasma density gradient in the near field of the antenna. Parasitic excitation of ion Bernstein waves may alter the profile of power deposition in fast wave heating experiments.

ACKNOWLEDGMENTS

We thank J. Taylor and W. Kineyko for technical assistance and R. Horton for providing the LaB_6 electron injector. One of us (F.S.) gratefully acknowledges many helpful discussions with Dr. T.H. Stix and Dr. M.D. Kruskal. This work supported by U.S. Department of Energy contract DE-AC02-76-CHO-3073.

REFERENCES

[1]E. Mazzucato, et al., Plasma Physics and Controlled Nuclear Fusion Research (London, 1984), IAEA (to be published).

[2]H. Park, N.C. Luhman, W.A. Peebles, and R. Kirkwood, Phys. Rev. Lett. 52, 1609 (1984).

[3]T.L. Owens, J.H. Mullen, F.W. Baity, W.A. Davis, O.C. Eldridge, and D.L. Hillis, Nucl. Fusion, 23, 49 (1983).

[4]M. Ono, F. Skiff, R. Horton, T. Watari, and K.L. Wong, Bull. Am. Phys. Soc., 28, 1126 (1983).

[5]P.L. Colestock and R.J. Kashuba, Nucl. Fusion, 23, 49 (1983).

[6]F. Skiff, M. Ono, R. Horton, and K.L. Wong, Bull. Am. Phys. Soc., 28, 1126 (1983).

[7]M. Ono, R. Horton, K. L. Wong, G. A. Wurden, and T. H. Stix, Bull. Am. Phys. Soc. 27, 967 (1982).

FIGURE CAPTIONS

Fig. 1 Coupling model.

Fig. 2 Results of coupling theory.

a. Coupling in uniform plasma.

b. Coupling with a density gradient in region II.

c. Dependence on parallel wave number.

d. Dependence on gradient scale length.

Fig. 3 Experimental setup.

Fig. 4 Identification of the ion Bernstein wave.

a. The sign of k_x is determined by plotting the in-phase vs quadrature component of the probe (with respect to antenna phase) as the probe is scanned.

b. Measured dispersion of the IBW.

c. IBW wave crests over a poloidal section.

Fig. 5 Density dependence.

a. Antenna loading vs edge density.

b. Density profile for lanthanum cathode.

c. Density profile for filament cathode.

Fig. 6 Effect of parallel wave number

a. 0° phasing

b. 180° phasing

Fig. 7 Wave amplitude profiles as a function of cathode emission current (density).

Fig. 8 Preference for steep gradient.

a. Wave interferograms over a poloidal section.

b. Density contours over a poloidal section.

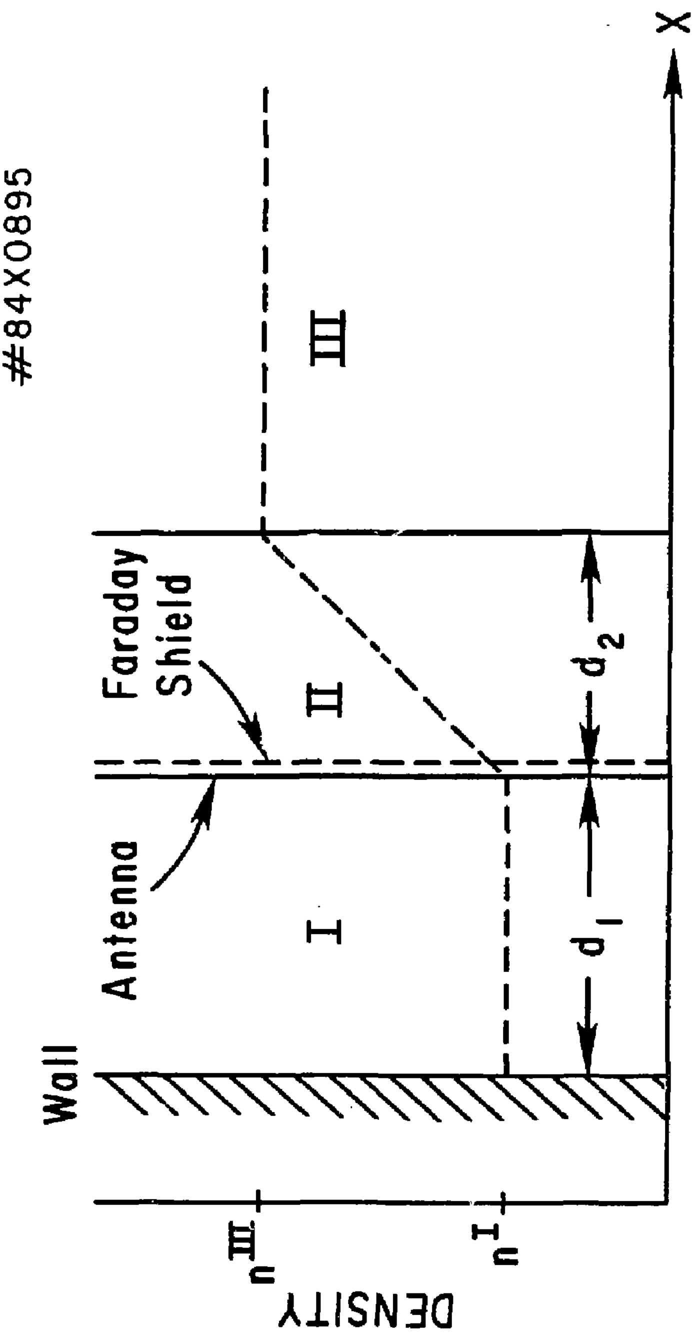
#84X0895
X
Faraday
Shield
Antenna
Wall
III
II
I
d_2
d_1
DENSITY
n_{III}
n_I

Fig. 1

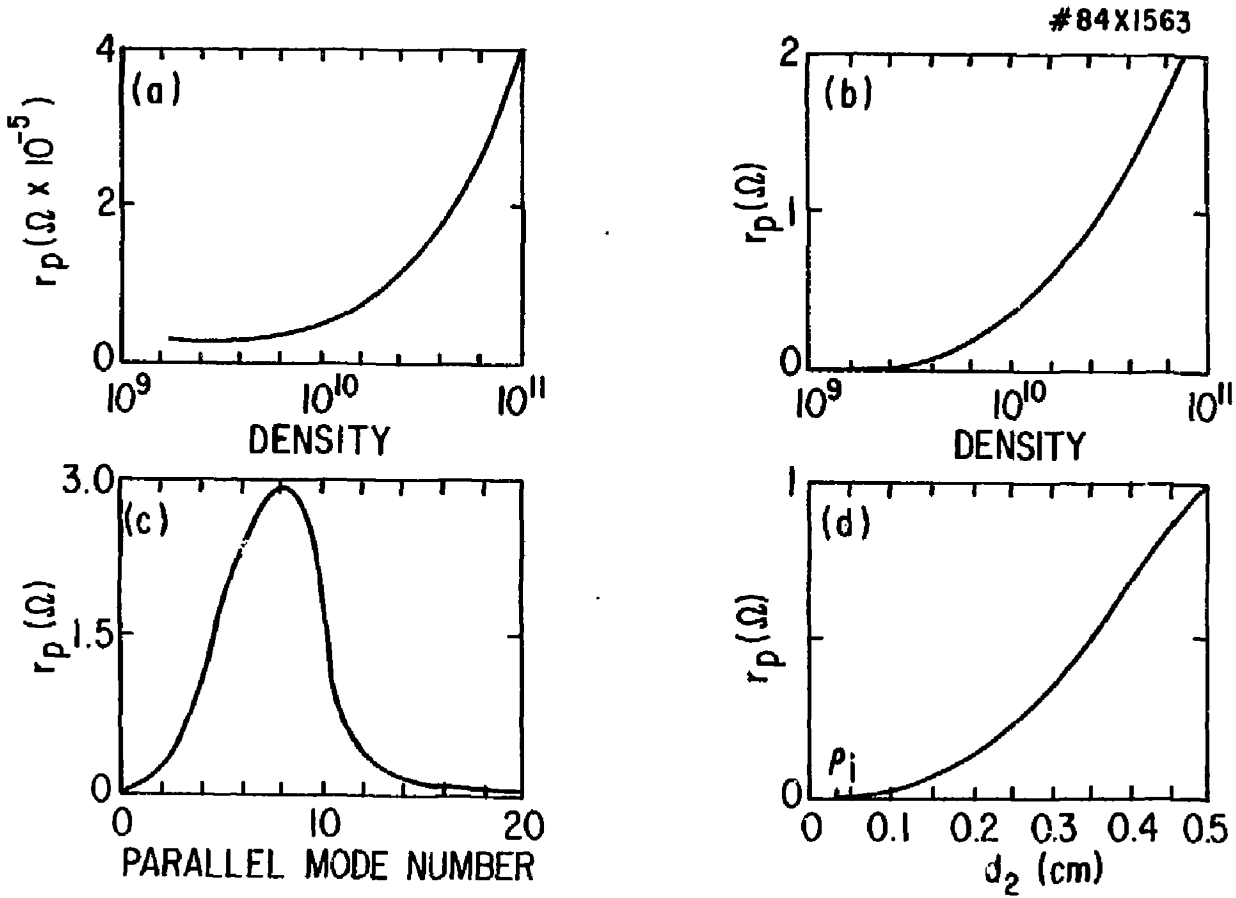
#84X1563
(a)
$r_p(\Omega \times 10^{-5})$
4
2
0
10^9
10^{10}
10^{11}
DENSITY
(b)
$r_p(\Omega)$
2
1
0
10^9
10^{10}
10^{11}
DENSITY
(c)
$r_p(\Omega)$
3.0
1.5
0
0
10
20
PARALLEL MODE NUMBER
(d)
$r_p(\Omega)$
1
0
ρ_i
0
0.1
0.2
0.3
0.4
0.5
d_2 (cm)

Fig. 2

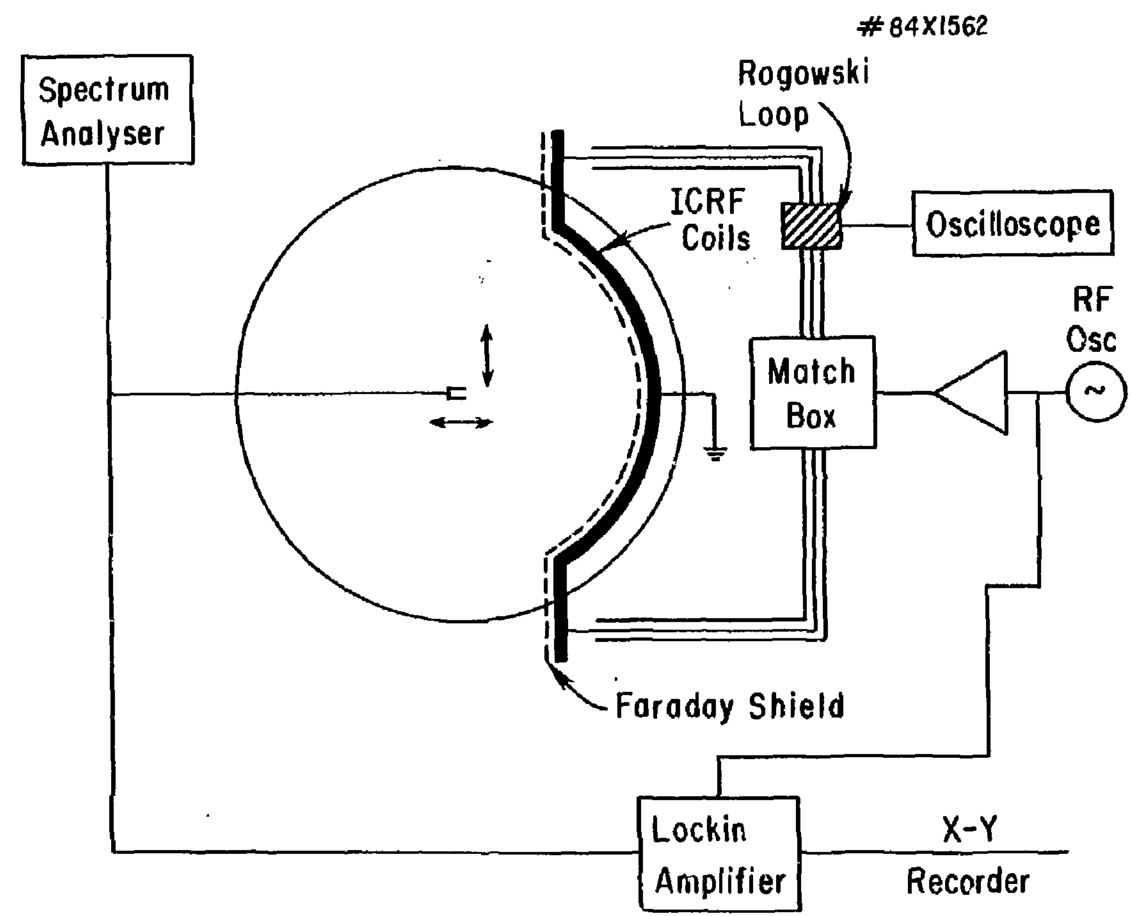

84X1562
Spectrum Analyser
Rogowski Loop
ICRF Coils
Oscilloscope
RF Osc
Match Box
Faraday Shield
Lockin Amplifier
X-Y Recorder

Fig. 3

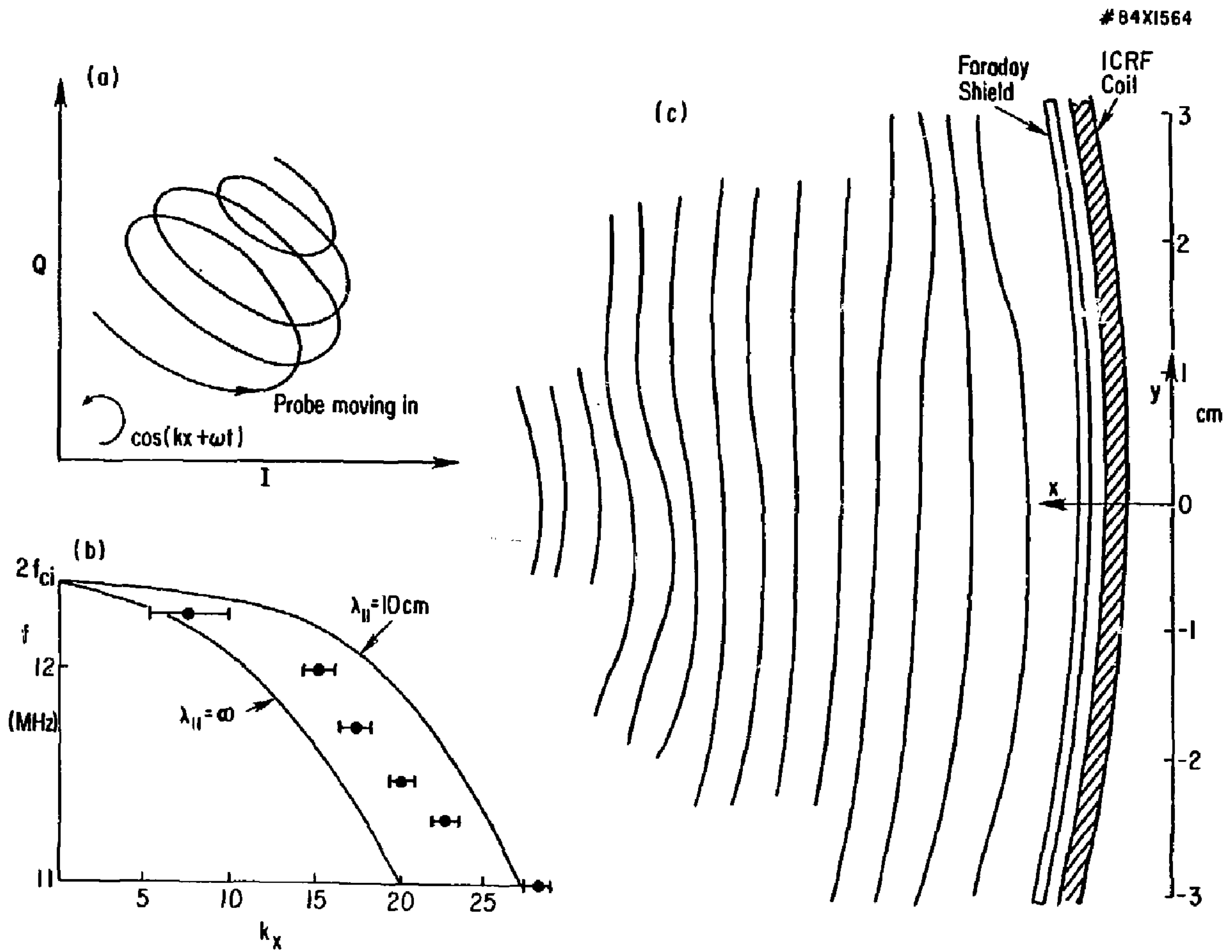
#84X1564
(a)
Q
I
Probe moving in
cos(kx+ωt)
(b)
2f_ci
f
12
(MHz)
11
λ∥=10cm
λ∥=∞
5
10
15
20
25
k_x
(c)
Faraday Shield
ICRF Coil
x
y
cm
3
2
1
0
-1
-2
-3

Fig. 4

#84X0940

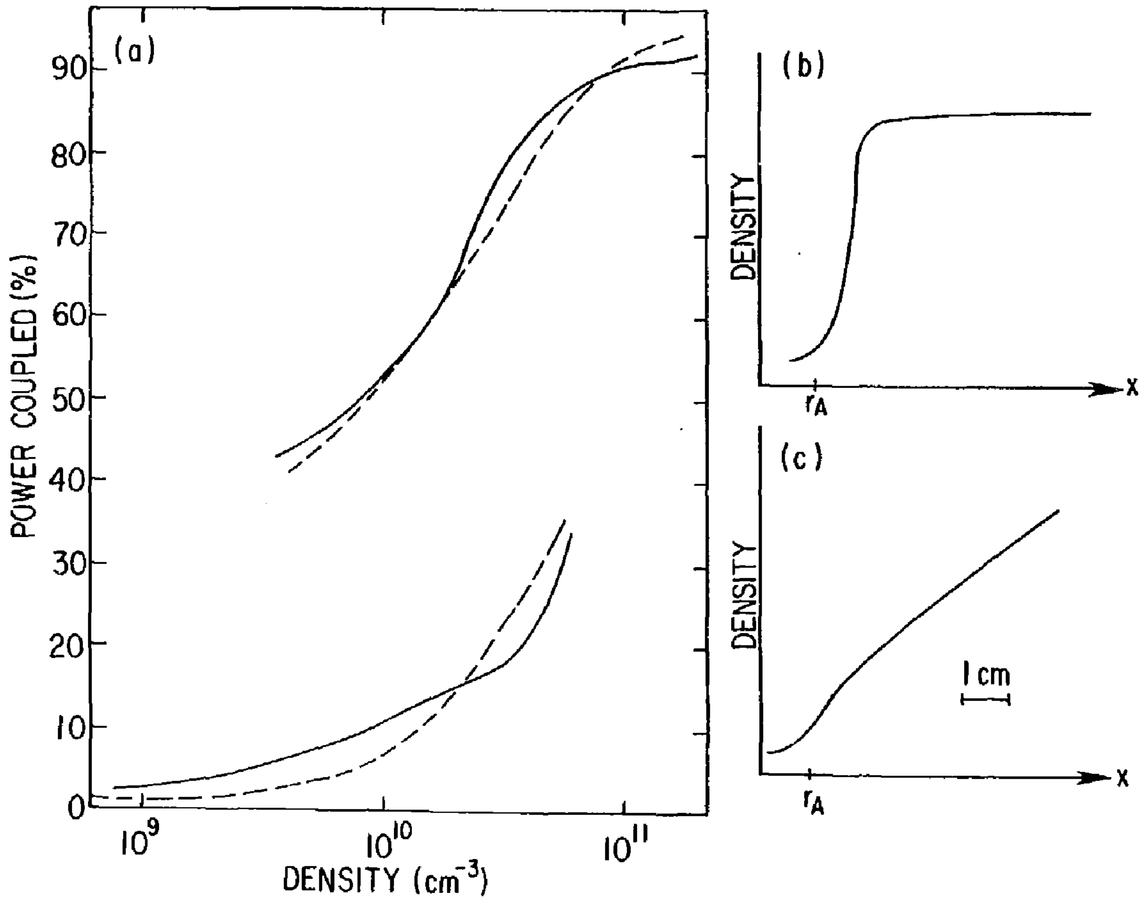

Fig. 5

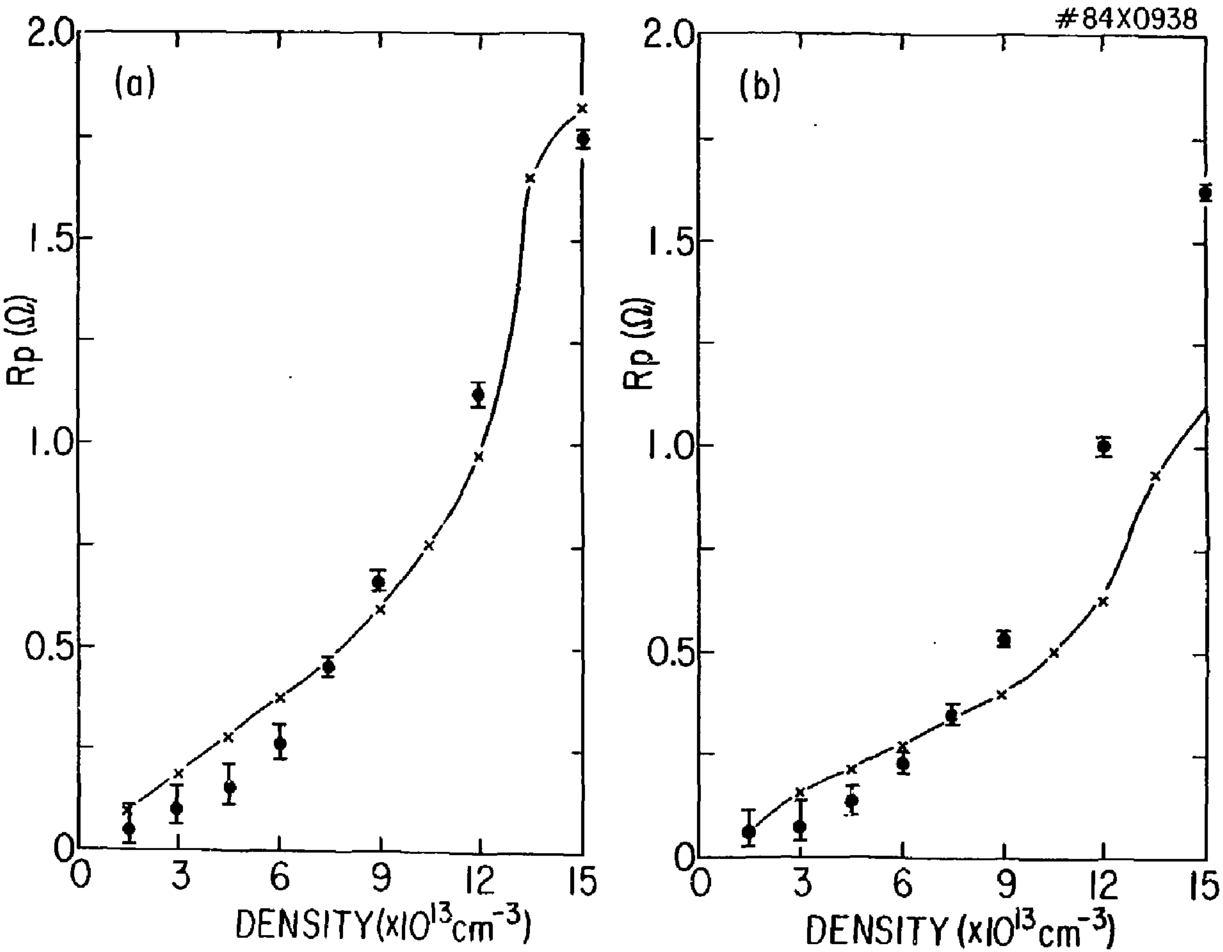

Fig. 6

#84X0941

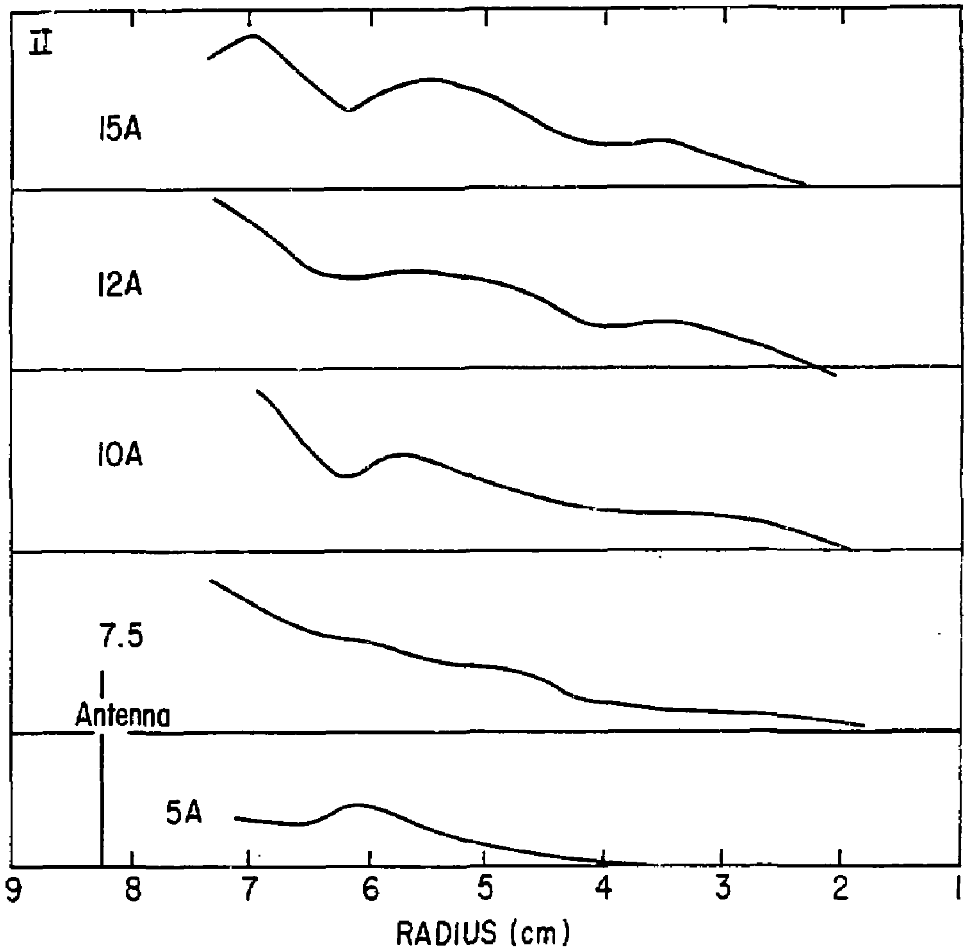

Fig. 7

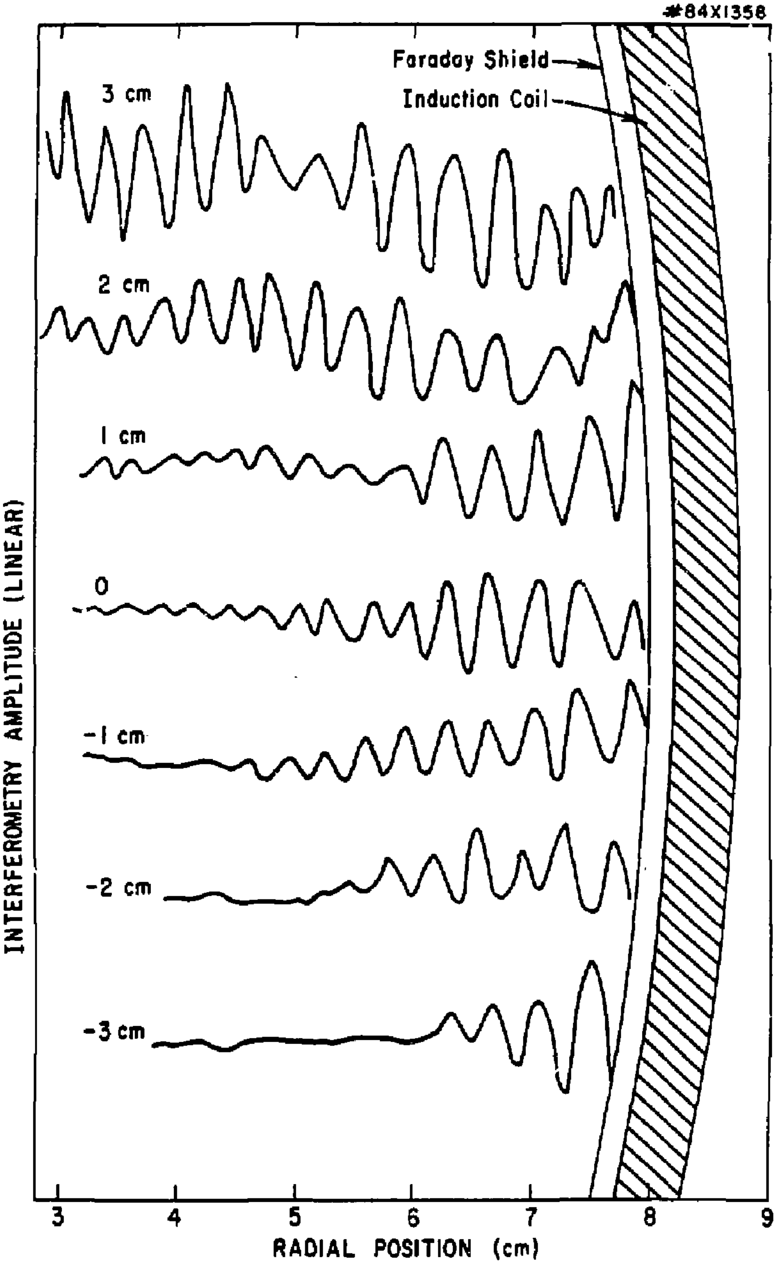
#84X1358
Faraday Shield
Induction Coil
3 cm
2 cm
1 cm
0
-1 cm
-2 cm
-3 cm
INTERFEROMETRY AMPLITUDE (LINEAR)
3
4
5
6
7
8
9
RADIAL POSITION (cm)

Fig. 8(a)

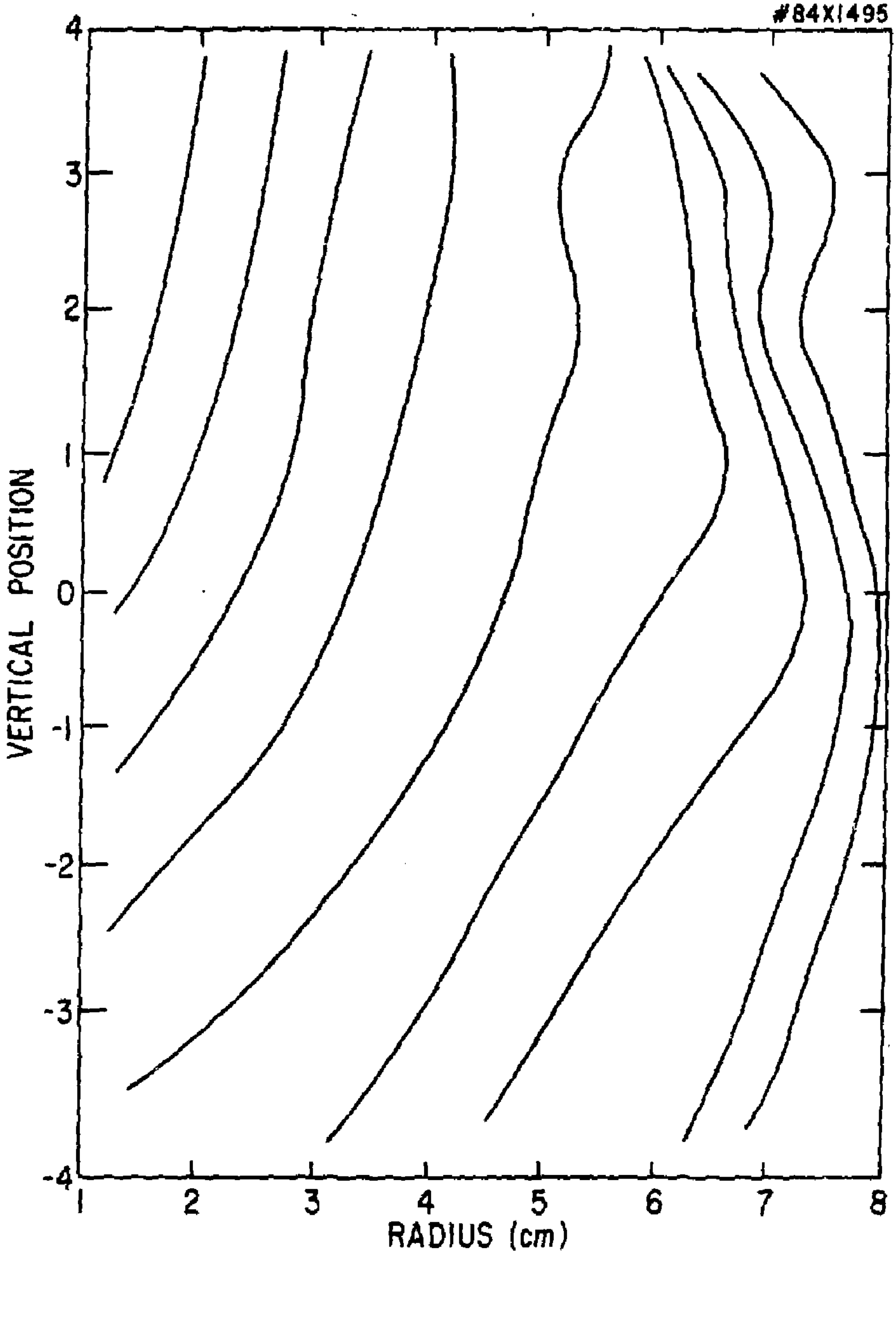

Fig. 8(b)

EXTERNAL DISTRIBUTION IN ADDITION TO TIC UC-20

Plasma Res Lab, Austra Nat'l Univ, AUSTRALIA
Dr. Frank J. Paoloni, Univ of Wollongong, AUSTRALIA
Prof. I.R. Jones, Flinders Univ., AUSTRALIA
Prof. M.H. Brennan, Univ Sydney, AUSTRALIA
Prof. F. Cap, Inst Theo Phys, AUSTRIA
Prof. Frank Verheest, Inst theoretische, BELGIUM
Dr. D. Palumbo, Dg XII Fusion Prog, BELGIUM
Ecole Royale Militaire, Lab de Phys Plasmas, BELGIUM
Dr. P.H. Sakanaka, Univ Estadual, BRAZIL
Dr. C.R. James, Univ of Alberta, CANADA
Prof. J. Teichmann, Univ of Montreal, CANADA
Dr. H.M. Skarsgard, Univ of Saskatchewan, CANADA
Prof. S.R. Sreenivasan, University of Calgary, CANADA
Prof. Tudor W. Johnston, INRS-Energie, CANADA
Dr. Hannes Barnard, Univ British Columbia, CANADA
Dr. M.P. Bachynski, MPB Technologies, Inc., CANADA
Zhengwu Li, SW Inst Physics, CHINA
Library, Tsing Hua University, CHINA
Librarian, Institute of Physics, CHINA
Inst Plasma Phys, Academia Sinica, CHINA
Dr. Peter Lukac, Komenskeho Univ, CZECHOSLOVAKIA
The Librarian, Culham Laboratory, ENGLAND
Prof. Schatzman, Observatoire de Nice, FRANCE
J. Radet, CEN-BP6, FRANCE
AM Dupas Library, AM Dupas Library, FRANCE
Dr. Tom Mual, Academy Bibliographic, HONG KONG
Preprint Library, Cent Res Inst Phys, HUNGARY
Dr. S.K. Trehan, Panjab University, INDIA
Dr. Indra, Mohan Lal Das, Banaras Hindu Univ, INDIA
Dr. L.K. Chavda, South Gujarat Univ, INDIA
Dr. R.K. Chhajlani, Var Ruchi Marg, INDIA
P. Kaw, Physical Research Lab, INDIA
Dr. Phillip Rosenau, Israel Inst Tech, ISRAEL
Prof. S. Cuperman, Tel Aviv University, ISRAEL
Prof. G. Rostagni, Univ Di Padova, ITALY
Librarian, Int'l Ctr Theo Phys, ITALY
Miss Clelia De Palo, Assoc EURATOM-CNEN, ITALY
Biblioteca, del CNR EURATOM, ITALY
Dr. H. Yamato, Toshiba Res & Dev, JAPAN
Prof. M. Yoshikawa, JAERI, Tokai Res Est, JAPAN
Prof. T. Uchida, University of Tokyo, JAPAN
Research Info Center, Nagoya University, JAPAN
Prof. Kyoji Nishikawa, Univ of Hiroshima, JAPAN
Prof. Sigeru Mori, JAERI, JAPAN
Library, Kyoto University, JAPAN
Prof. Ichiro Kawakami, Nihon Univ, JAPAN
Prof. Satoshi Itoh, Kyushu University, JAPAN
Tech Info Division, Korea Atomic Energy, KOREA
Dr. R. England, Civdad Universitaria, MEXICO
Bibliotheek, Fom-Inst Voor Plasma, NETHERLANDS
Prof. B.S. Liley, University of Waikato, NEW ZEALAND
Dr. Suresh C. Sharma, Univ of Calabar, NIGERIA
Prof. J.A.C. Cabral, Inst Superior Tech, PORTUGAL
Dr. Octavian Petrus, ALI CUZA University, ROMANIA
Prof. M.A. Hellberg, University of Natal, SO AFRICA
Dr. Johan de Villiers, Atomic Energy Bd, SO AFRICA
Fusion Div. Library, JEN, SPAIN
Prof. Hans Wilhelmson, Chalmers Univ Tech, SWEDEN
Dr. Lennart Stenflo, University of UMEA, SWEDEN
Library, Royal Inst Tech, SWEDEN
Dr. Erik T. Karlson, Uppsala Universitet, SWEDEN
Centre de Recherchesen, Ecole Polytech Fed, SWITZERLAND
Dr. W.L. Weise, Nat'l Bur Stand, USA
Dr. W.M. Stacey, Georg Inst Tech, USA
Dr. S.T. Wu, Univ Alabama, USA
Prof. Norman L. Oleson, Univ S Florida, USA
Dr. Benjamin Ma, Iowa State Univ, USA
Prof. Magne Kristiansen, Texas Tech Univ, USA
Dr. Raymond Askew, Auburn Univ, USA
Dr. V.T. Tolok, Kharkov Phys Tech Ins, USSR
Dr. D.D. Ryutov, Siberian Acad Sci, USSR
Dr. G.A. Eliseev, Kurchatov Institute, USSR
Dr. V.A. Glukhikh, Inst Electro-Physical, USSR
Institute Gen. Physics, USSR
Prof. T.J. Boyd, Univ College N Wales, WALES
Dr. K. Schindler, Ruhr Universitat, W. GERMANY
Nuclear Res Estab, Julich Ltd, W. GERMANY
Librarian, Max-Planck Institut, W. GERMANY
Dr. H.J. Kaeppler, University Stuttgart, W. GERMANY
Bibliothek, Inst Plasmaforschung, W. GERMANY